Norwegian Meteorological Institute

METreport

No. 05/2021
ISSN 2387-4201
Free

Norwegian standard climate normals 1991-2020 - the methodological approach

Ole Einar Tveito

Norwegian Meteorological Institute

METreport

Title Norwegian standard climate normals 1991-2020- the methodological approach	**Date** August 25, 2021
Section Division for Climate Services	**Report no.** 05/2021
Author(s) Ole Einar Tveito	**Classification** ● Free ○ Restricted
Client(s)	**Client's reference**

Abstract

Standard climate normals are reference values used for monitoring climate anomalies, providing information about which conditions that could be expected at a specific locations. They are based on averages of 30-year observation series. Up to now the standard normal reference period has been 1961-1990. It will now be replace by the period 1991-2020 in order to get reference values that is more consistent with the current climate conditions.

During the last 20-30 years the observation network has been modernised and drastically changed. The new standard station normals are therefore calculated from a set of *homogenised* time series where effects of re-locations, change of equipment etc have been adjusted. Methods are developed to fill gaps in series that are not complete in the entire 30-year period. For weather stations having less than 15 years of observations, monthly standard normals are estimated applying a anomaly gridding approach

Gridded maps of the monthly normal values are established using a combination of station normals and information of regional gradients from the SeNorge gridded daily data.

Keywords

precipitation , gap filling, interpolation, homogenisation

Disciplinary signature
Hans Olav Hygen

Responsible signature
Cecilie Stenersen

Contents

1 Introduction

Climate normals are climate reference values, used for climate monitoring, societal planning, estimation of design values, etc., making the society well prepared for climate and weather impacts. The practices and guidelines for climate normals are described by the World Meteorological Organisation, *WMO* (2018, 2017). WMO recommends to use a 30-year period as reference, and this has been the international practise since the first standard normals were published in the 1930-ies, based on 1901-1930 as reference period. The standard normals presented in this report are the fourth generation of normals, following the periods 1901-30,1931-60 and 1961-90. The definition of reference periods are official WMO guidelines, securing consistent reference periods all over the world. Up to now consecutive thirty year periods (1901-30,1931-60, 1961-1991 and 1991-2020) have been used as normal periods. WMO has recently changed this practise (*WMO*, 2017), and from now on the standard climate normals will be updated every 10 year to represent the most recent 30-year period finishing in a year ending with 0. This new practise will ensure that the climate normals reflects the recent climate conditions, which is important in periods where climate is changing.

Climate monitoring requires long term observation series of high and known quality. The observation series should ideally be homogeneous and complete, taken at the same location with the same instrumentation and in an unchanged environment throughout the observation period. This demand is however very, and maybe, too ambitious. The reality is that the meteorological observation network is constantly changing both with respect to instrumentation, observation practices, location of the stations and changes in the natural and built environment surrounding the stations. This means that observation series evidently are disrupted and incomplete. WMO recommends that for calculation of a normal value for a month data should be available for at least 80% of the years within the averaging period (*WMO*, 2018, 2017). In addition, the period without data should not exceed three consecutive years, but this criterion is considered not to be very strict. However, in periods and regions where there is a strong temporal trend in the data series, this is an issue that must be considered.

Since normal reference values are also required at locations and for observation series not fulfilling the most strict requirements of WMO, MET Norway has decided to esti-

mate normals also for stations with quite short observation series. This is a challenge since it will require extensive interpolation and/or extrapolation of data for the periods where observations are missing. The meteorological observation network in Norway has undergone drastic changes and modernisation during the last thirty years. Stations are automated, providing data more frequently and in real time. During automatisation many stations are relocated, and/or equipment and sensors are changed. During the period 1991-2020 the number of stations observing temperature has increased, while the precipitation network, dominated by manual rain observations, has decreased. Also the data retrieval and the data quality control systems have been changed and modernised. A consequence is that there are many incomplete observation series, or series that are not continuous throughout the entire thirty-year period. In this report the approaches and analyses that are used to derive the new climate normals for Norwegian weather stations are presented. The methods applied to derive the 1991-2020 normals presented here reflects the data availability, the need for spatial and temporal interpolations, and the challenge of representing the trends in the observation series in light of the ongoing climate change. The new 1991-2020 standard normals replace the 1961-90 standard normal values for percipiation (*Førland*, 1993) and temperature (*Aune*, 1993).

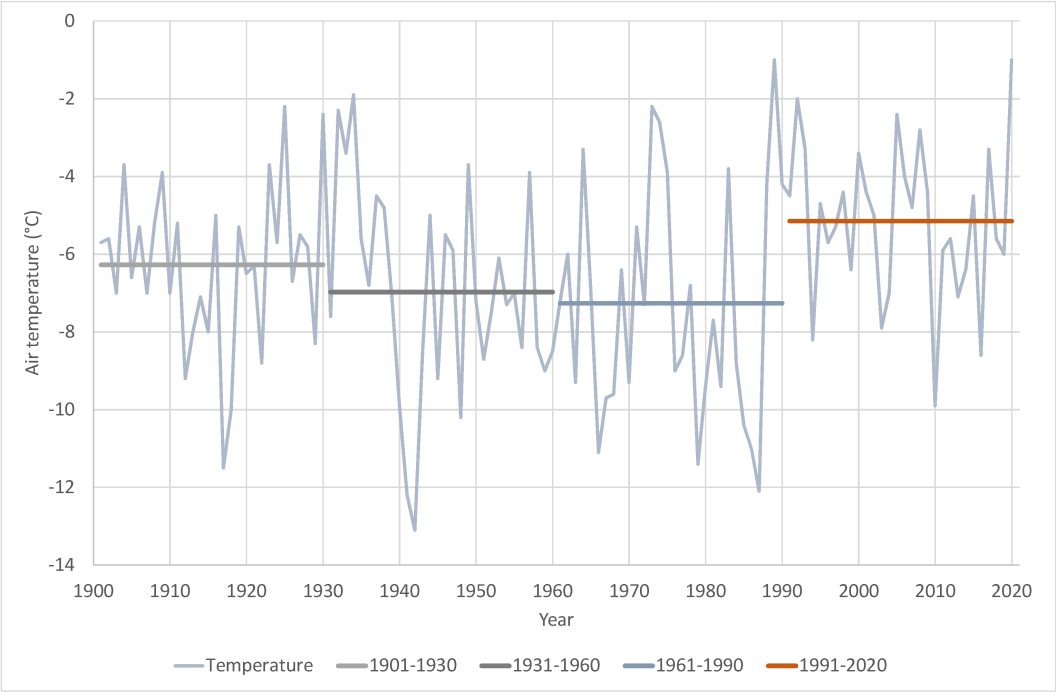

Figure 1: Averaged mean monthly temperature in January for Norway, 1901-2020. The horizontal lines represent the standard normal periods 1901-30,1931-60, 1961-90 and 1991-2020 respectively.

2 Background

Climate is not stationary in time. During the last 120 years we have now had four consecutive standard climate normal period. Figure 1 shows the variability of the average January air temperature for Norway the last 120 years. The four averages for the standard normal periods are marked as horizontal lines. During the first three periods the temperature was showing a slightly decreasing trend. For the most recent thirty years the average jumps up more than 2 degrees, reflecting the strong warming signal that has been present since the late 1980s. The new climate normal period for the period 1991-2020 is thus strongly influenced by the ongoing global warming. Such a strong trend in the climate underpin the need for a new, and more representative climate reference value representing the expected weather (and climate).

When analysing trends in observation series it is important that the series are homogeneous and only represent trends and changes in the weather and climate. Observation series can be severely influenced by external factors such as relocations, change of instruments, change of observers and/or observation practices and changes in the environment near the station. The latter include buildings, land use and vegetation. These external factors might introduce an inhomogeneity in the series, either as an abrupt shift or as a gradual change. The first type of inhomogeneity is often caused by relocation, new equipment or new building nearby. Removal of vegetation close to the sensors is also a cause in this category. When vegetation is growing or the land-use is gradually changing the inhomogeneity will appear slowly, as a trend.

The first type of inhomogeneities are relatively easy to detect and adjust. There are a number of well tested methods developed for this purpose. The most applied methods for homogenisation in Europe are HOMER (*Mestre et al.*, 2013), ACMANT (*Domonkos*, 2019) and SNHT (*Alexandersson*, 1986). The SNHT method is implemented in the *Climatol* (*Guijarro*, 2018) R-package for analysing climate data. The second type is more difficult to identify and compensate for.

The effect of the homogenisation can easily be illustrated by comparing maps of the change of monthly normal values between 1961-1990 and 1991-2020 based on "raw" unhomogenised series with maps based on homogenised series for January (Figure 2). Such anomaly maps should appear as smooth fields representing just temporal climate variations when averaged over a sufficient long time period. The homogenised data set shows such a smooth change, representing regional climate trends, while the raw data result in a map with local variations implying local inhomogeneities at some of the stations. The maps based on homogenised data are clearly more trustworthy in explaining the large-scale climate variations that should explain the change in the "normal" climatology.

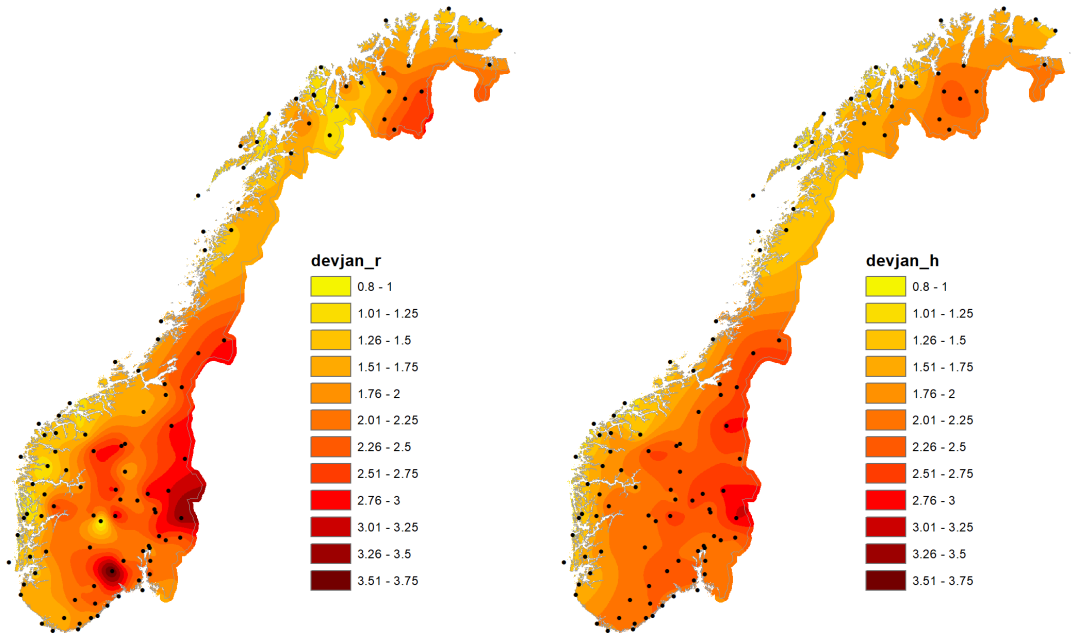

(a) Unhomogenised data.

(b) Homogenised data.

Figure 2: The effect of homogenisation on the difference between the 1961-1990 and 1991-2020 mean monthly January temperature.

3 Temperature

3.1 Homogenised reference data set

The primary data basis for deriving the monthly standard normal values in Norway are 108 homogenised data series (Figure 3) covering the period 1961-2018. These series are tested and homogenised (*Kuya et al.*, 2020) applying HOMER (*Mestre et al.*, 2013). In the analysis series from Sweden and Finland were included to make the analysis of series near the national borders more robust. Only nine of the Norwegian series were found homogeneous throughout the entire 1961-1990 period. The most common reasons for inhomogeneities were relocations (43.8% of the breaks), automation (14.4%), new instruments (13%), new radiation screen (13%) and painting of radiation screen (9.1%). In the homogenisation only breaks that are justified by metadata and station history are adjusted. For the calculation on normal values 1991-2020 the homogenised series are updated up to 2020. Homogeneity breaks that may have been introduced after 2018 are not analysed nor compensated for.

3.2 Reconstruction of periods with data gaps

Not all the series used by *Kuya et al.* (2020) have complete series throughout the analysis period. In the homogeneity analysis gaps in the data series are filled by algorithms implemented in the homogeneity analysis tools. Even though they serve the purpose for providing complete dataseries for the homogenisation, these methods are not sufficiently transparent with respect to data tracking and reproducibility. An alternative method for estimating missing values in the time series tracking all estimates is therefore implemented.

This method is quite simple. It is based on linear relations between the series having missing values (predictand series) and the complete neighbouring (predictor) series with the highest correlations with the predictand series. The three highest correlated predictor series are used for the estimations. The linear model is expressed as

$$\hat{X} = a + \sum_{i=1}^{3} b_i Y_i \tag{1}$$

where a and b_i are coefficients, $\hat{X}$ is the series to be predicted, and Y_i are the predictor series.

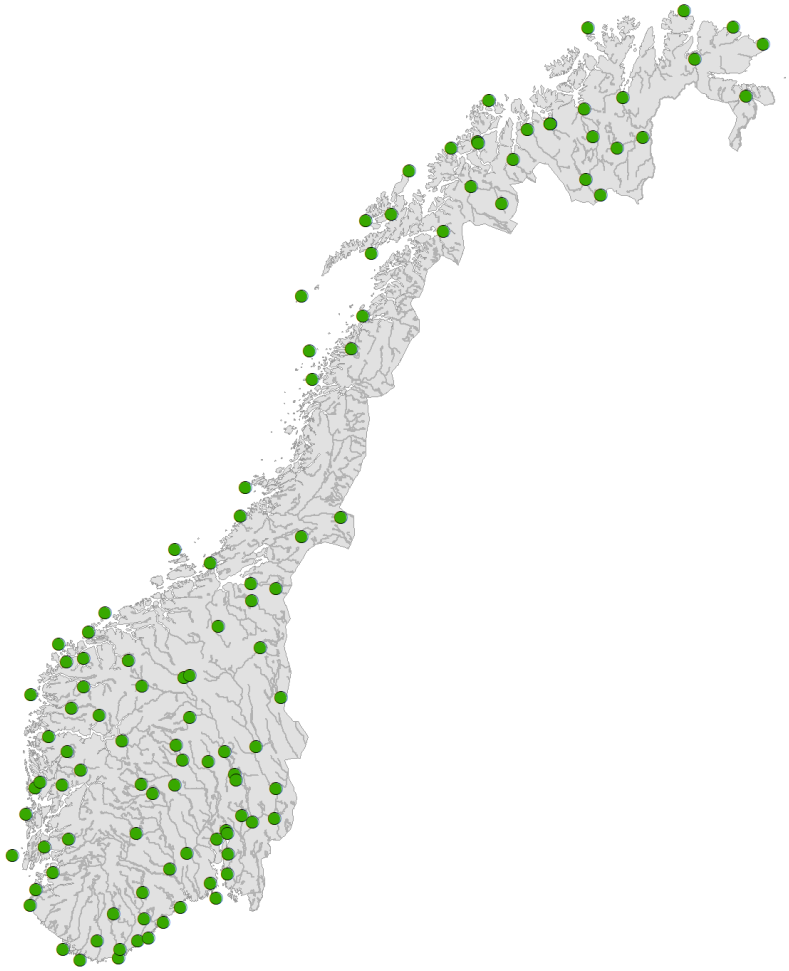

Figure 3: The location of the 108 homogenized temperature series (*Kuya et al.*, 2020)

To avoid the influence of seasonality, both the predictand ($\hat{X}$) and the predictor series (Y_i) are normalised on a monthly level before fitting the linear model. The normalisation takes this form for the predictand series:

$$X_{nm} = X_m - \overline{X_m} \tag{2}$$

where X_{nm} are normalised monthly values and $\overline{X_m}$ are the monthly mean values in the calibration period.

The predictors are normalised only for the period(s) where the predictand have data. This is to prevent that false trends are introduced in the back transformation to absolute (non-normalised) predicted series. It is therefore urgent that both the predictand and predictor series are normalised over the same data periods. Normalisation of predictor series will thus follow

$$Y_{nm} = Y_m - \overline{Y_m} \mid X \neq \emptyset \tag{3}$$

The linear model to estimate X_n then becomes

$$\hat{X_n} = a + \sum_{i=1}^{3} b_i Y_{n_i} \tag{4}$$

This ensures that any trends deviating from the calibration period (the period where X have data) are represented by the predictor series. Since the Y_{n_i}s are complete series is $\hat{X_n}$ a complete estimate for the entire period 1961-2020. The predicted series is achieved by a backtransformation by adding the monthly mean values of the calibration period ($\overline{X_m}$).

The procedure is iterative, so the series with less and shortest gaps are completed first. The reconstructed complete series are then included in the predictor data for filling gaps in remaining series with gaps. The justification for this is that the number of missing values for most of these series are low, and randomly distributed throughout the period 1961-2020, however with some more gaps in the start and end of the period.

The final reconstructed series is a combination of original and homogenised values. The reconstructed series were re-homogenised. No further homogeneity breaks are identified within the 1961-2018 period that was analysed in *Kuya et al.* (2020).

3.3 Calculation on monthly temperature normals

The approach to calculate new standard normal values is a three step procedure

1. *Missing observations in the homogenised series are estimated by linear regression to complete the series*. 108 series covering the period 1961-2020 are included in this step. The interpolated series are reinvestigated to check if new inhomogeneities are introduced. This is not the case, except for possible homogeneity breaks within the last years of the series that was not considered in the analysis by *Kuya et al.* (2020). Detected homogeneity breaks in the first and last 4-5 years of the series are considered as uncertain, and normally not adjusted.

2. Additional series with *more than 15 years* of observations are completed by linear regression. The predictors are the three most correlated series with the target series among the 108 homogenised series from step 1. Additional 59 series are made complete in this step.

3. Series shorter than 15 years are reconstructed by extracting monthly anomalies from a gridded data set of monthly deviations from the 1991-2020 normal value based on a spatial interpolation of monthly anomalies of the 167 series from step 1 and 2 for the period 1991-2020. The extracted deviations are used in a re-engineering approach to estimate a complete time series combining the anomaly values and existing observations.

3.4 Extending the reference data set

The 108 homogenised series do not represent the total potential for series with sufficient data coverage for calculating 1991-2020 normal since it was focusing on the period covering both the 1961-1990 and 1991-2020 normal periods. Homogenisation will be more robust when a longer data period is analysed, and by analysing the entire 1961-2020 period a homogenised data basis for studying the changes between the two recent normal periods was established.

Further *59* series have more than 15 years of data within the 1961-2020 period. Fifteen years time series are considered to be a sufficient large data sample to establish a reasonably robust linear model for estimating missing values in a monthly times series.

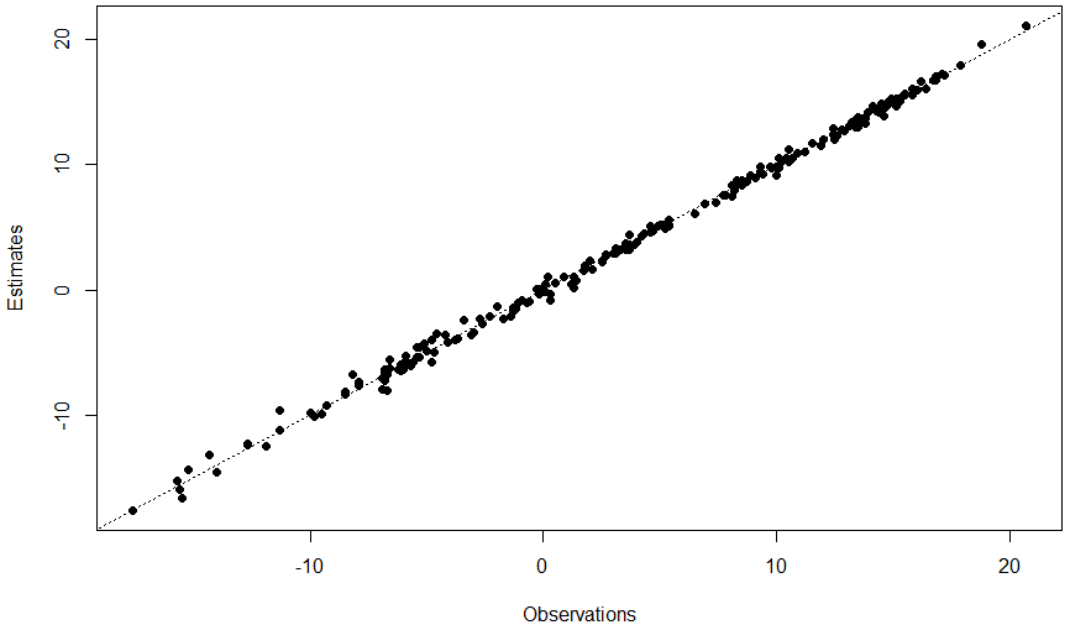

Figure 4: Observed vs. estimated temperature in the linear model for 12180 Ilseng.

If not complete, the missing values in these time series are estimated by the same linear model procedure as described above, with the exception that the reconstructed series are not added back to the calibration data. The estimated series are validated through statistics for the linear model fit, and traditional validation scores like bias and root mean square error. Figure 4 and 5 shows the results of the estimation for the arbitrary selected series 12180 Ilseng. The station has data from 1961 until January 1972, and thereafter, with some gaps, since March 2013. The linear model for this station has a coefficient of determination of 0.98. The median bias at this station is low (range -0.1 - 0.23), but as seen in figure 6 the variation in estimation biases is large. The RMSE is therefore as high as 0.43.

3.5 Construction of monthly normal values at locations with short data series

For observation series shorter than 15 years, there is high a risk that single values have a large influence on the mean value. Prediction of series using simple linear models as described above is therefore not recommended. There is still however a need for estimating climate normal values also at these locations. The applied approach is based on a spatial interpolation of monthly residuals similar to the one used to produce the maps in the

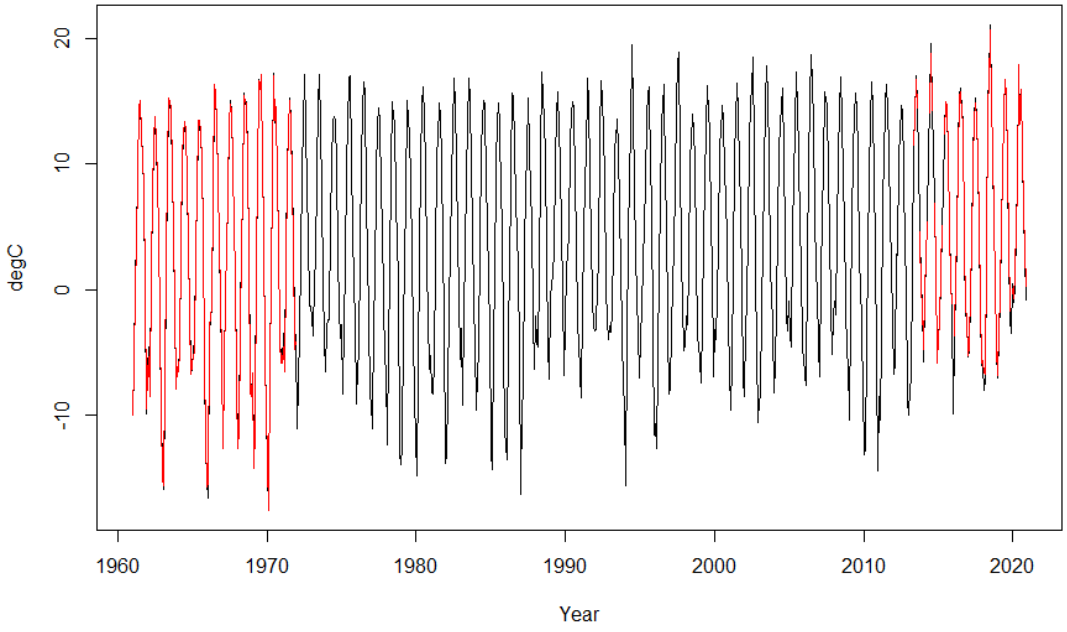

Figure 5: Estimated monthly temperature series by a linear model for the weather station 12180 Ilseng for the period 1961-2020. The red line represents the observed values, the black curve represents the modelled temperature values.

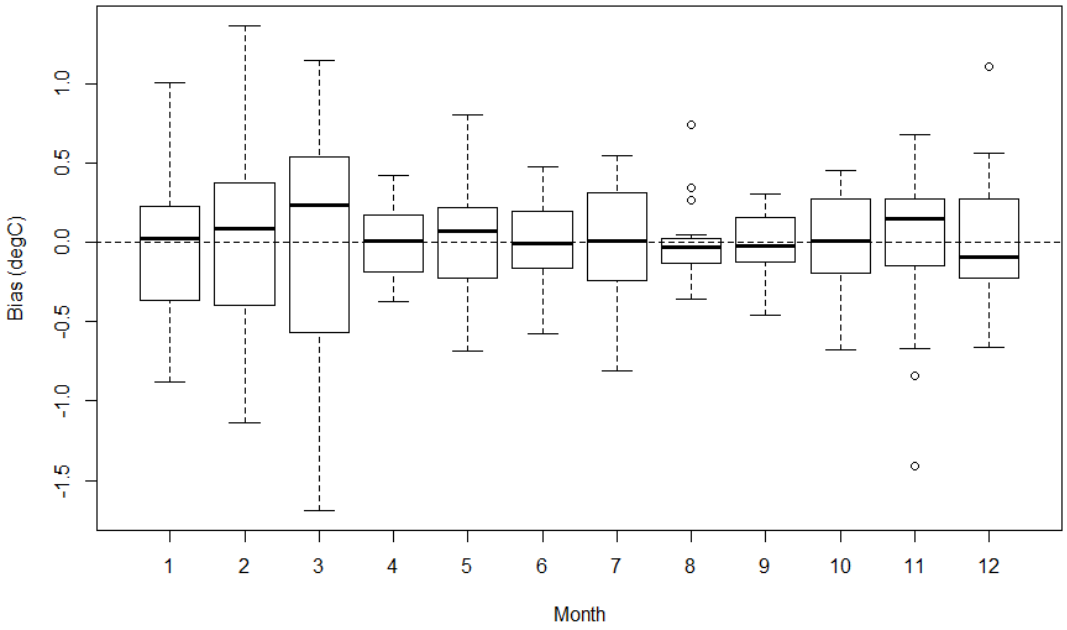

Figure 6: Monthly biases for the estimated monthly temperature series by a linear model for 12180 Ilseng

monthly climate monitoring reports issued by MET (https://www.met.no/publikasjoner/met-info).

Monthly residual grids with 1 x 1 km spatial resolution for the period 1961-1990 is derived from the monthly anomaly from the 1991-2020 mean values applying the Topo to Raster algorithm (*Hutchinson*, 1989) implemented in ArcGIS. This is essentially a discretized thin plate spline technique (*Wahba*, 1990) for which the roughness penalty has been modified to allow the fitted digital elevation model (DEM) to follow abrupt changes in terrain, such as streams, ridges and cliffs. By interpolating the monthly residuals the second-order stationarity assumption that is expected for most spatial interpolation methods is likely to be met. By second-order stationarity we assume that the co-variance between two points is the same for a given distance and direction, not depending on the choice of points.

At the input point locations the interpolated monthly anomaly grids will produce an unbiased estimate. The monthly anomalies represent deviations from the expected clima-

tology. For each of the target series a 30 year time series of climate anomalies is projected from the monthly anomaly grids. These anomaly estimates are then combined with the few observations that exist in a reverse engineering approach to calculate the 1991-2000 mean values following this equation.

$$\hat{T_N} = \frac{\sum_{i=1}^{n}(\hat{bias}_i + T_i)}{n} \tag{5}$$

If the anomaly gridding is representative, the variance of the estimated monthly values are small. This is usually the case where the station network is well distributed, and there are a few years of observations. In areas where the station network is sparse, or the climate variations are large, the estimates will show larger variations. There is also a clear signal that the series with longer observation records achieve more stable estimates than short series, since the impact of single weather events will be reduced.

For the anomaly gridding the 167 reconstructed series are applied. Gridded time series of monthly anomalies for the 1961-2020 period are estimated, but only the 1991-2020 period is applied to calculate the 1991-2020 monthly mean values. Calculations are done when the series has more than two observations for each calendar month.

By applying this approach mean monthly values for 385 more stations are calculated. In contradiction to the homogenised and reconstructed series presented in step 1 and 2 only the long term average value is kept as result from the anomaly gridding step.

In the end, monthly standard normal temperatures for the 1991-2020 period are estimated for 552 station series in Norway (Figure 7).

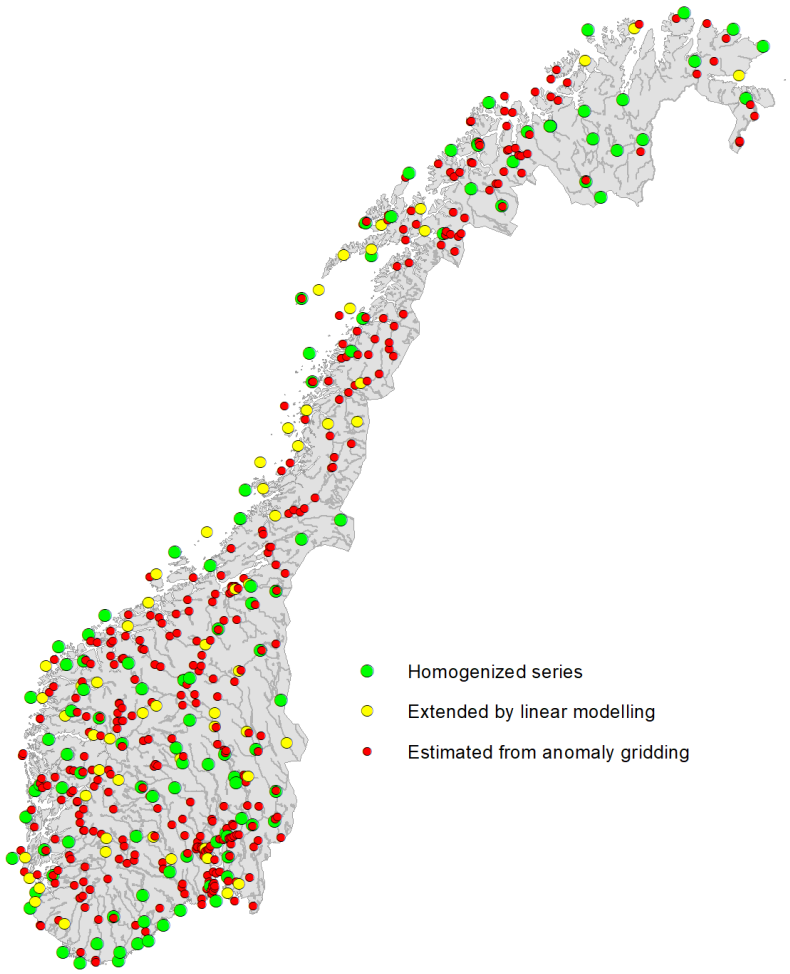

Figure 7: The location of the temperature series for which standard normal values are estimated. The colours indicate the approach used to achieve the data basis for the normal value calculations

4 Gridded normal temperature maps 1991-2020

The normal temperatures derived by the steps described above have been used to establish gridded maps for monthly normal temperatures 1991-2020. Temperature has a strong altitude dependence, that will vary with regions, season and the actual weather situation. Using the "rule of thumb" of a decrease of 0.65°C pr. 100 m elevation increase will e.g. result in temperatures that are far too cold in the mountains during winter since the coldest temperatures occur during inversion situations where the temperature will increase with elevation. This is demonstrated by *Tveito et al.* (2000) where a linear regression of mean monthly temperatures with several different predictors including different elevation parameters showed that the vertical temperature gradient was smallest during the winter season. *Tveito et al.* (2000) applied one vertical temperature gradient for the entire Fennoscandia. In this analysis we apply regional temperaure gradients derived from the newly developed SeNorge2018 daily gridded dataset (*Lussana et al.*, 2019). Here are the vertical temperature gradient is estimated from the actual observations, using both horizontal and vertical distances as criterias for the interpolation. For the calculation of the *mean vertical temperature gradients* all the possible combinations of vertical temperature differences within a 11 x 11 km window around each grid cell in the SeNorge grid are calculated. To avoid the influence of flat areas (sea and lakes) are the temperatures for grid cells with the same elevation averaged. The vertical temperature gradient for the central grid point is assigned through a linear fit to all the possible temperature elevation differences when at least 60 unique combinations are present, and that the maximum elevation range in those combinations exceed 100 meters.

The gridded normal temperatures are estimated by residual kriging. Instead of reducing the temperatures to sea level as proposed by *Tveito et al.* (2000) the temperatures are reduced to a smoothed elevation level representing the 50 km mean elevation shown in Figure 8b. Stations having very different characteristics than neighbouring stations are removed from from the analysis before the point values are interpolated into a 1 x 1km grid using ordinary kriging. Examples of stations that are removed are mountain top stations like 31970 Gaustatoppen and 97710 Iskoras II.

The interpolation of monthly temperature grids is carried out as follows. First all the station temperatures are reduced to the *reference level*, the 50 km smoothed elevation:

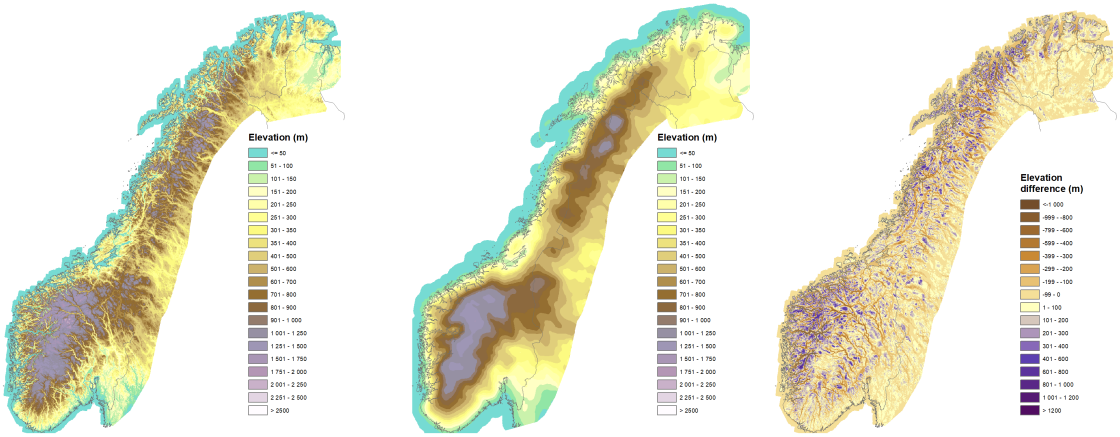

(a) Elevation model 1 km. (b) Elevation model 50 km. (c) Elevation difference between 1 and 50 km DEM

Figure 8: The elevation models used in calculation of gridded temperature normal maps.

$$T_{50km} = T - (Z - Z_{50km}) \cdot dtdz \tag{6}$$

where Z_{50km} is the 50 km elevation at the station, Z is the station elevation and $dtdz$ is the monthly mean vertical temperature gradient for the station gridcell. After the spatial interpolation the following post processing is carried out on the grids:

$$\hat{T}_{1km} = T_{ref} + (DEM_{1km} - DEM_{50km}) \cdot dtdz \tag{7}$$

where T_{ref} is the the interpolated(gridded) temperature at reference level, DEM_{1km} and DEM_{50km} are the 1 km and 50 km elevation models respectively, and $dtdz$ the gridded vertical temperature gradient field. Figure 9 shows the map of mean annual temperature. Maps of mean monthly temperatures are presented in the figure 10.

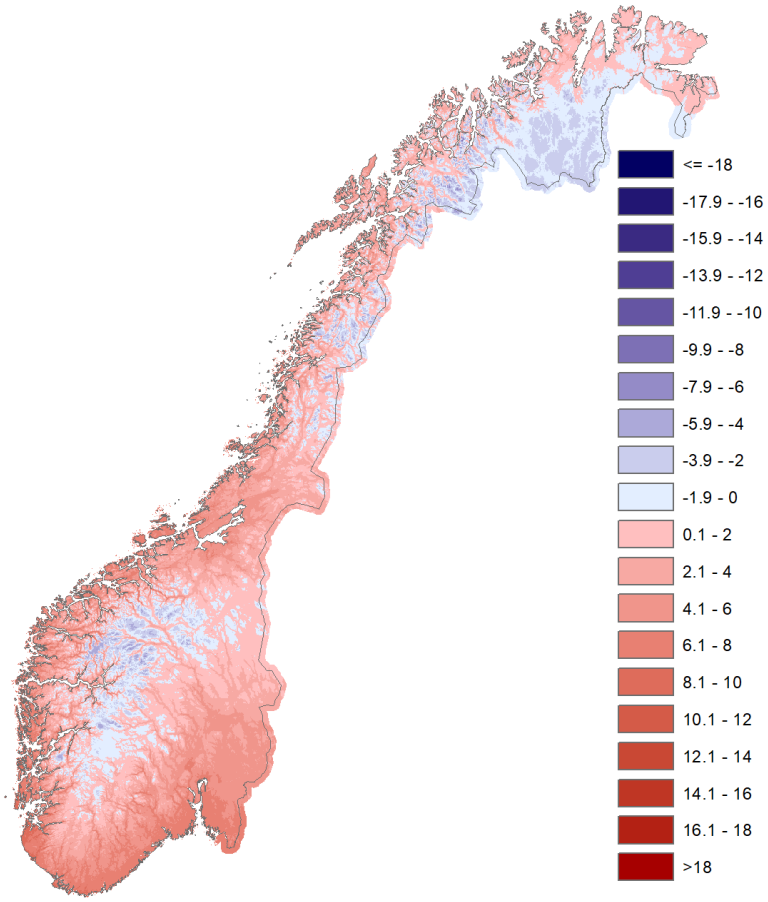

Figure 9: Mean annual temperature 1991-2020

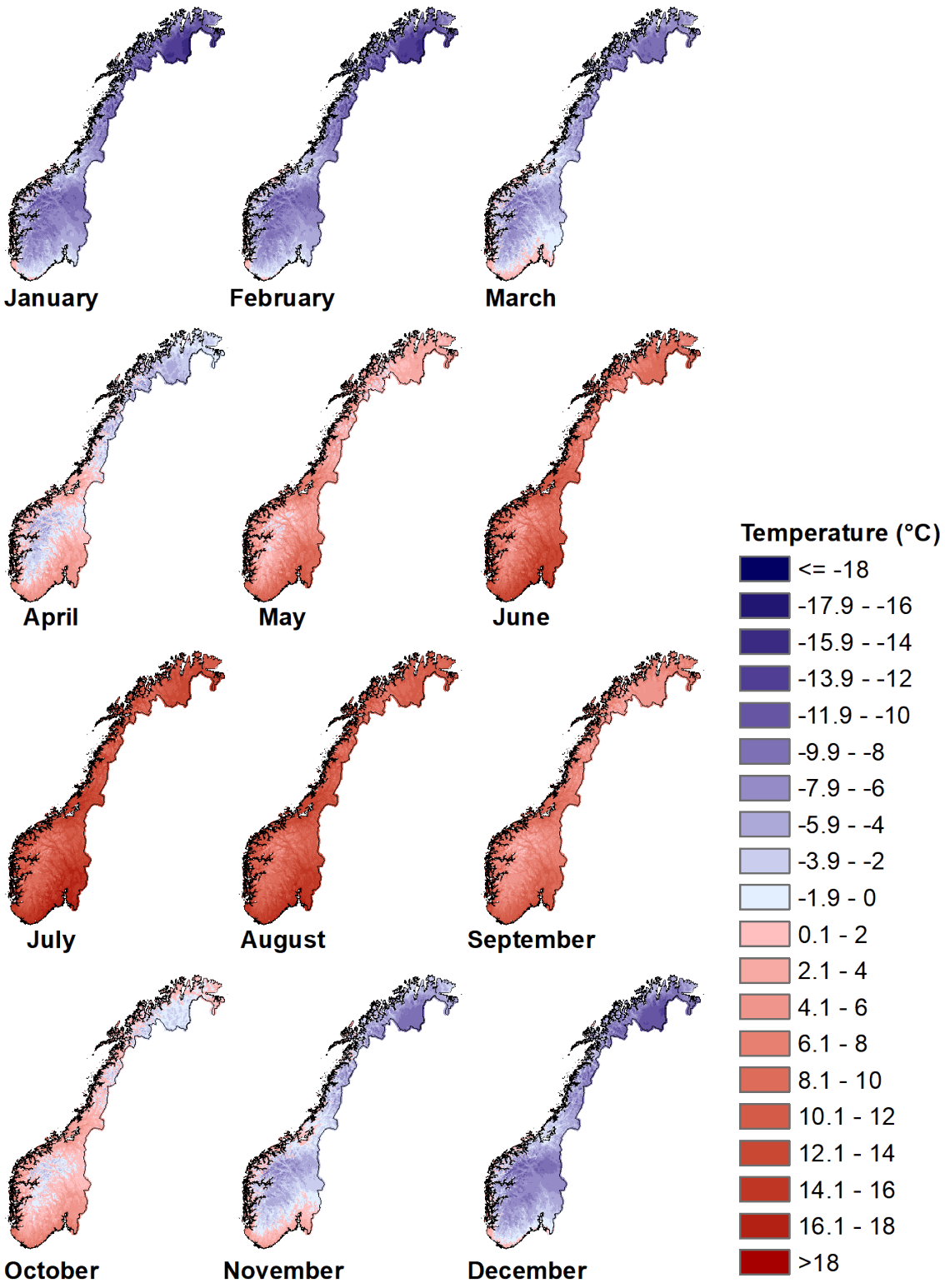

Figure 10: Mean monthly temperatures 1991-2020

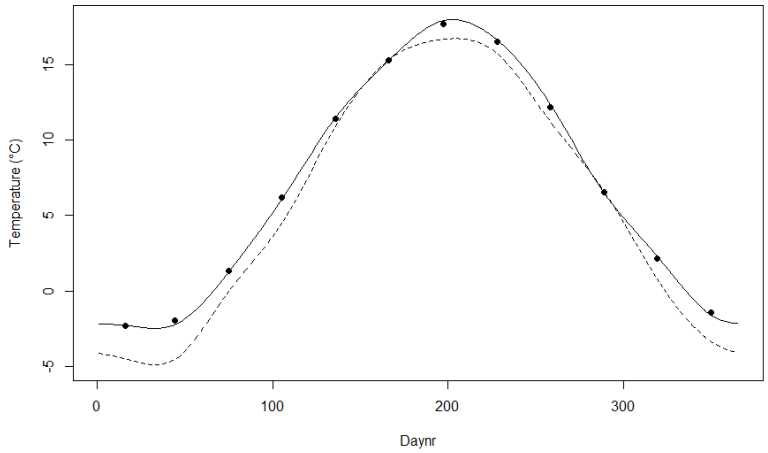

Figure 11: Daily normal temperatures (curve) and mean monthly temperatures (dots) 1991-2020 at 18700 Oslo-Blindern. The dashed line represents the daily normal temperatures for the 1961-1990 period.

5 Daily temperature normal values

In order to determine temperature seasons and degree-days, daily normal values have to be estimated. This is achieved by interpolating daily values from the monthly normal temperatures applying a cubic spline algorithm (see e.g *Press et al.* (1992)). In the approach applied here, a constraint was added to the spline equation. This constraint ensures that the deviation between the gridded monthly mean temperature and the mean monthly temperature based on the daily (splined) values are within an acceptable tolerance (0.001 °C is used). The amplitude of the spline curve was adjusted by shifting the positions of the monthly mean (default in the middle of the month). This was done iteratively until the tolerance criterion was fulfilled (S.L.Lystad, pers.comm., *Tveito et al.* (2001)). This method reproduces the observed daily thirty year means quite well as shown in figure 11. In this graph, showing the daily normal temperatures for the 18700 Oslo-Blindern station is also the daily normal temperatures for the old normal period 1961-1990 is presented, showing the seasonal variation of the observed temperature change.

In figure 11 we see that the temperature change is largest in winter, and smallest in late spring and in autumn.

6 Precipitation, data and methods

Normal values are calculated for the mean monthly precipitation sum for the period 1991-2020. The basis for the calculations is the set of 325 *homogenized* monthly precipitation series for the period 1961-2020 presented by *Kuya et al.* (2021). These series are either single site series from one location only, or series that are merged from precipitation stations at different locations within a short distance. Most of these stations were relocated within the period.

As for temperature these 325 homogenized series do not provide a complete coverage for the entire 1961-2020 period. Only 42 of the series are 100% complete For the homogenization of precipitation the R-package *climatol* (*Guijarro* (2018)) was applied. In that process, missing values were interpolated by averaging values from neighbouring stations. In order to provide documented and traceable interpolated values, the missing values provided by *climatol* were replaced by values estimated by a linear regression. This is the same procedure as used for temperature. To avoid estimates of negative precipitation is the square root of monthly precipitation is analysed. The two most correlated complete precipitation series to the series to be interpolated are used as predictors. The series with fewer gaps are filled first, and can be applied as predictor series once they are complete. The coefficient of determination is higher than 0.9 for more than half of the series with gaps.

For the remaining series the anomaly gridding approach is applied. Monthly precipitation anomaly grid (in percent of the monthly normal values) based on the 325 homogenized stations is derived using the *TopoGrid* algorithm presented in section 3.5. The gridded anomalies are extracted at 1183 locations where precipiation stations have been in operation. The re-einginering approach is applied to retrieve the normal value based on the ratio between the existing observations at the stations and the monthly residual. At least two values for each month within the 1991-2020 is required to establish the relation needed to establish a time series. In the end, 1089 stations, including the original 325, are assigned with normal values. The derived normals are checked manually by plotting the station values in a map. Suspect values are inspected, and for six of the stations the estimated normals are rejected. The main reason for rejecting the estimated normal values is poor data wuality or non-representative observations.

7 Gridded normal precipitation maps 1991-2020

The gridded normal maps are derived using a similar approach that is used in SeNorge v1.1 (*Tveito et al.*, 2005). It assumes that precipitation has an elevation dependence. In SeNorge this dependence is 10%/100m and comes in addition to a correction for gauge undercatch (windloss). Evaluation of these values e.g. through hydrological modelling indicate that the SeNorge1.1 precipitation is overestimated, especially in the high elevation areas. In this analysis the observations are not corrected for the undercatch, and the elevation dependence is set to 7%/100m, which is closer to the elevation dependency suggested by *Førland* (1979).

The spatial interpolation is carried out applying inverse distance weighting (IDW), including the eight nearest stations. IDW takes only the distance between observations points into account. As for SeNorge1.1, two 1 x 1 km grids are derived. One grid with precipitation and one with elevations calculated from the altitude of the stations. The final normal grids are calculated as

$$\hat{RR} = RR_0 + 0.007 \cdot (DEM - DEM_{rr}) \tag{8}$$

where RR_0 is the interpolated precipitation grid, DEM is the 1 x 1 km elevation model and DEM_{rr} is the interpolated elevation grid from the precipitation station altitudes. Figure 12 shows the annual precipitation in Norway in the period 1991-2020. The maximum annual precipiation value is 6130 mm in the area of Ålfotbreen on the west coast, and the minimum value 212 mm is estimated for a small area in Saltdal in Nordland. The monthly precipitaion normal grids are shown in figure 13.

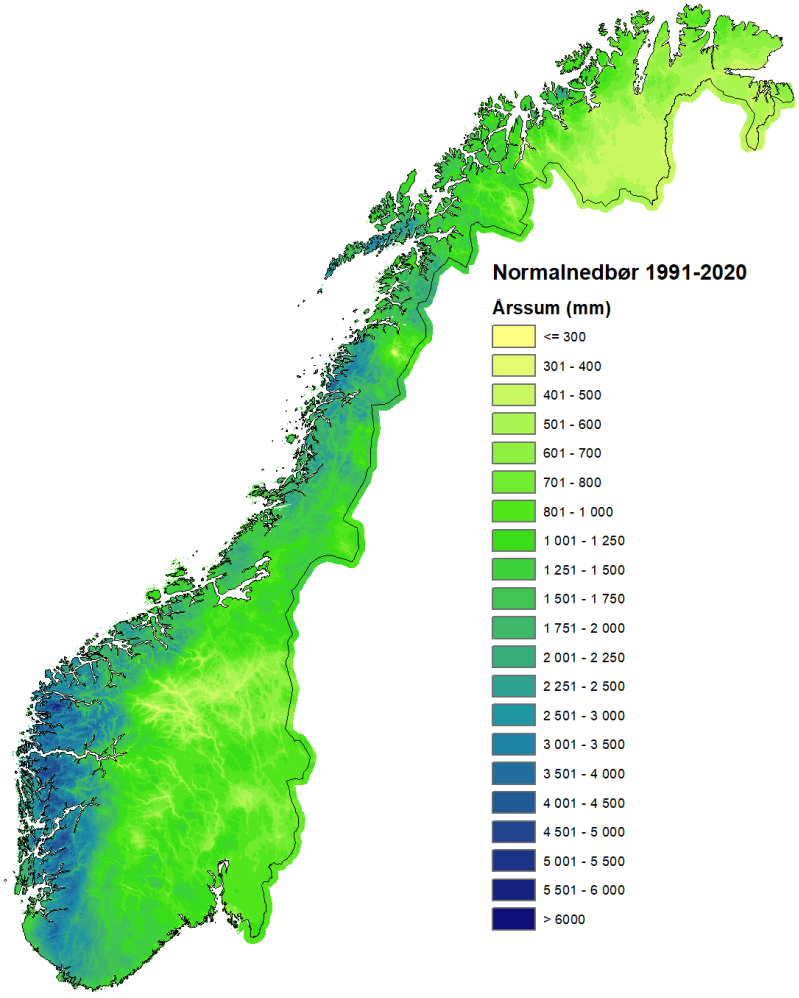

Figure 12: Mean annual precipitation 1991-2020

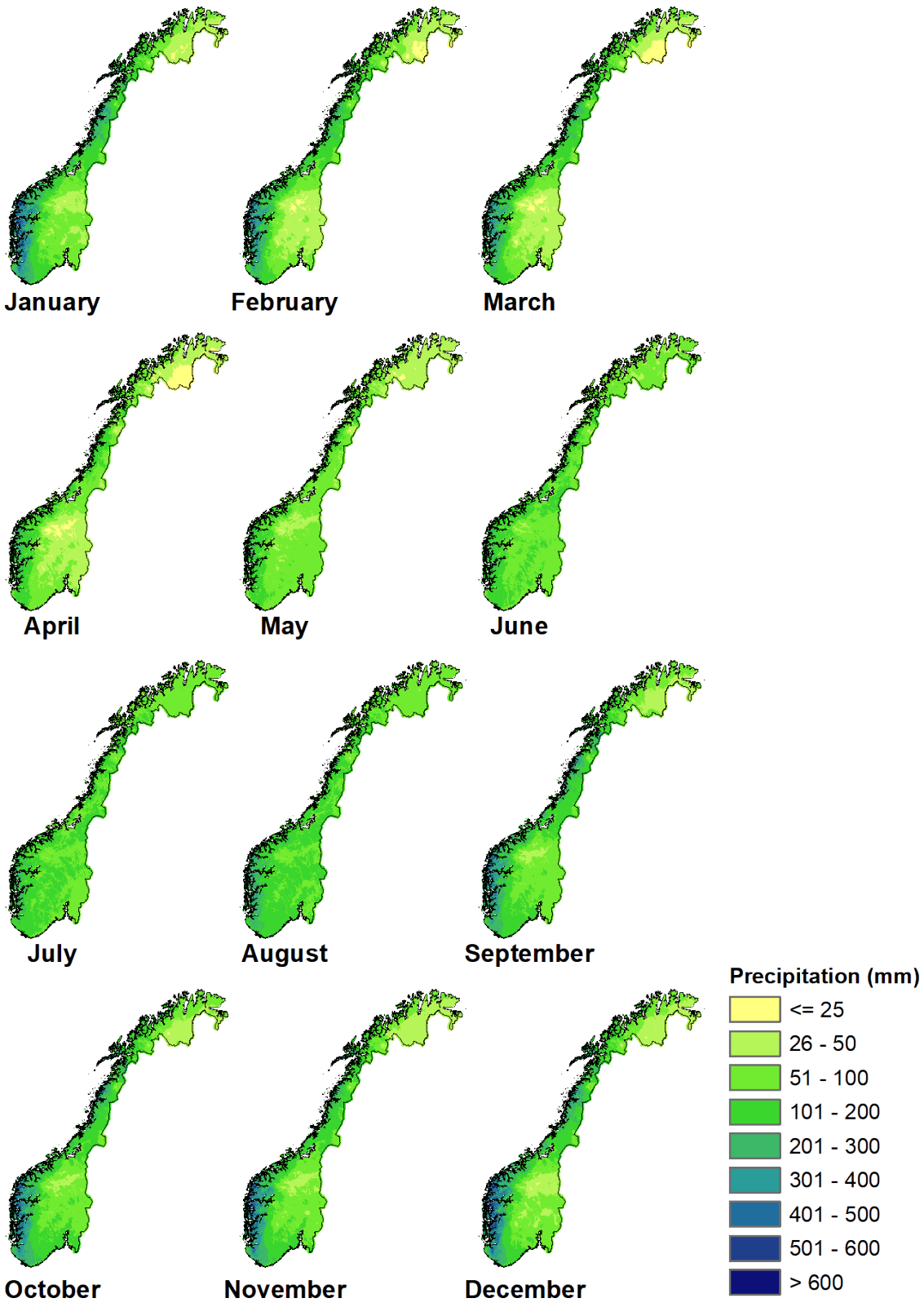

Figure 13: Mean monthly precipitation 1991-2020

8 Changes from the 1961-1990 normal values

As shown in figure 14 the mean annual temperature in Norway has increased in the recent decades. In the preceding three standard normal periods the difference between the thirty year periods are small compared to the change in the last thirty years. The figure shows that only a few years in the last thirty year period have annual mean temperatures below the old 1961-90 normal. If the seasonal temperatures are considered (Figure 15), we notice differences in the trends between the seasons. The temperature increase is absolutely largest in the winter season, and less in summer. Alls easons are warmer in the recetnt 30-year period comapred to the 1961-90 normal period.

The temperature change also differs with regions. In general, the temperature is increases most in the inner parts of the country, like Finnmarksvidda and in the inner parts of southeastern Norway, mostly due to the winter warming. On an annual basis (Figure 16) has the temperature increased most in southeastern Norway and in eastern Finnmark. There are large regional differences in the seasonal temperature change (Figure 17). The smallest change has occurred along the west coast, in the high mountains near Sognefjord and in Finnmark in summer and autumn. In spring the strongest warming is observed around the Oslofjord and in Eastern Finnmark. The strongest warming signal has occurred in winter, with an increase of more than 2.5 degrees in southeastern Norway.

Precipitation also shows an increasing trend through the last 120 years (figure 18). The largest annual change have occurred between the two most recent normal periods. Compared to the most recent normal period has the precipitation increased in all seasons, except autumn (figure 19). Maps of the regional changes reveal that the increase is largest in winter and spring. In winter the increase is largest in southwestern Norway, in spring along the northwest coast. In summer parts of northern Norway has become drier, while inner parts of southern Norway have experienced the largest increase in precipitation . Autumn has become drier literally all over the country.

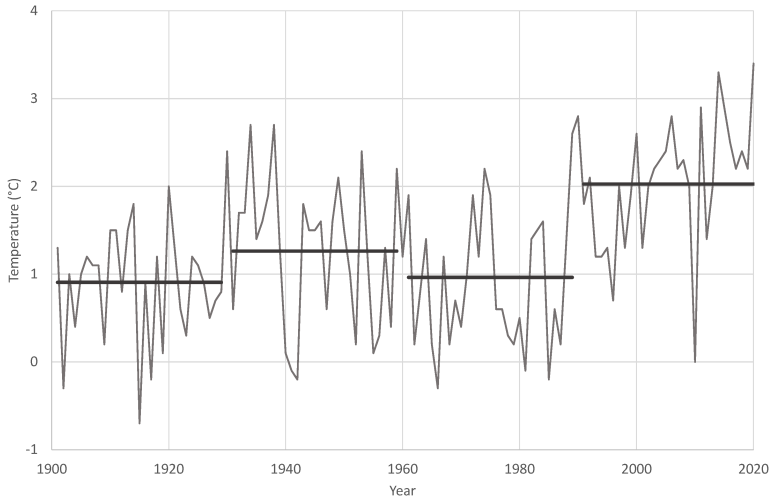

Figure 14: Average mean annual temperature in Norway 1901-2020. The horizontal lines represent the consecutive 30 year average (normal) values 1901-1930,1931-60, 1961-90 and 1991-2020.

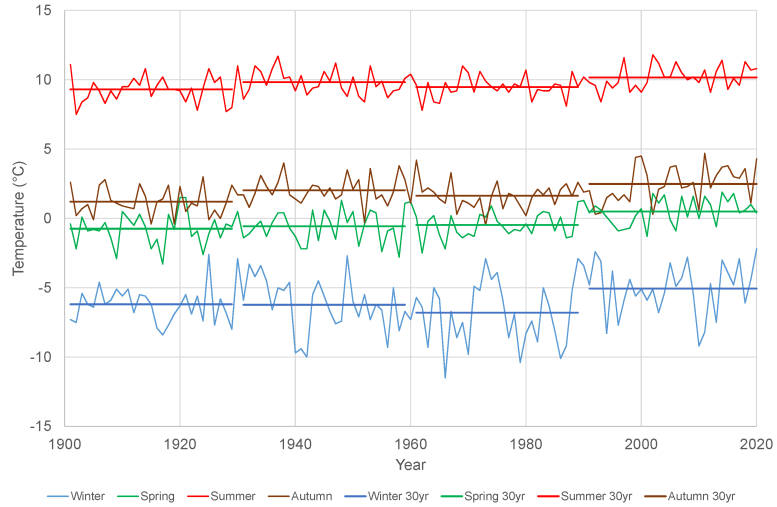

Figure 15: Average mean seasonal temperatures in Norway 1901-2020. The horizontal lines represent the consecutive 30 year average (normal) values 1901-1930,1931-60, 1961-90 and 1991-2020.

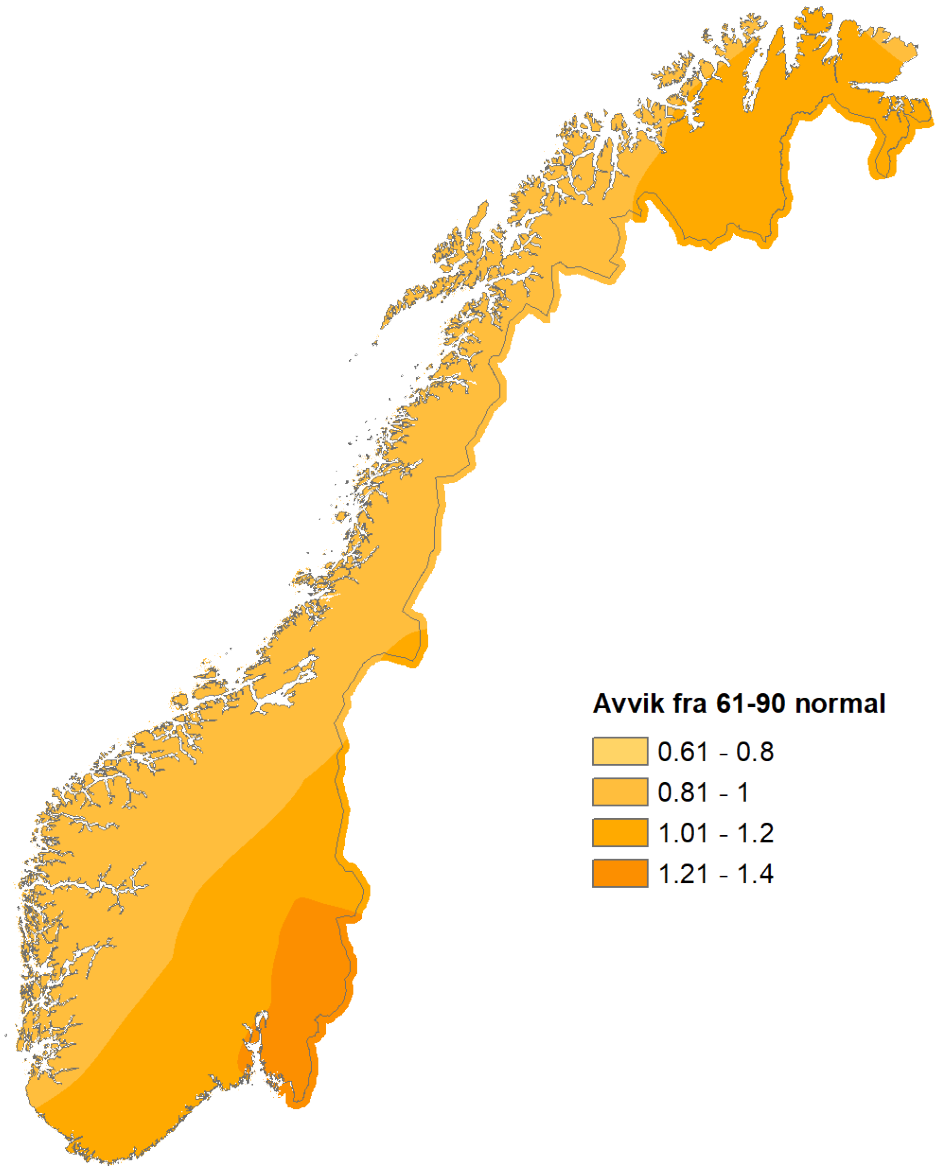

Figure 16: The difference between mean annual temperature in the period 1991-2020 and the period 1961-1990.

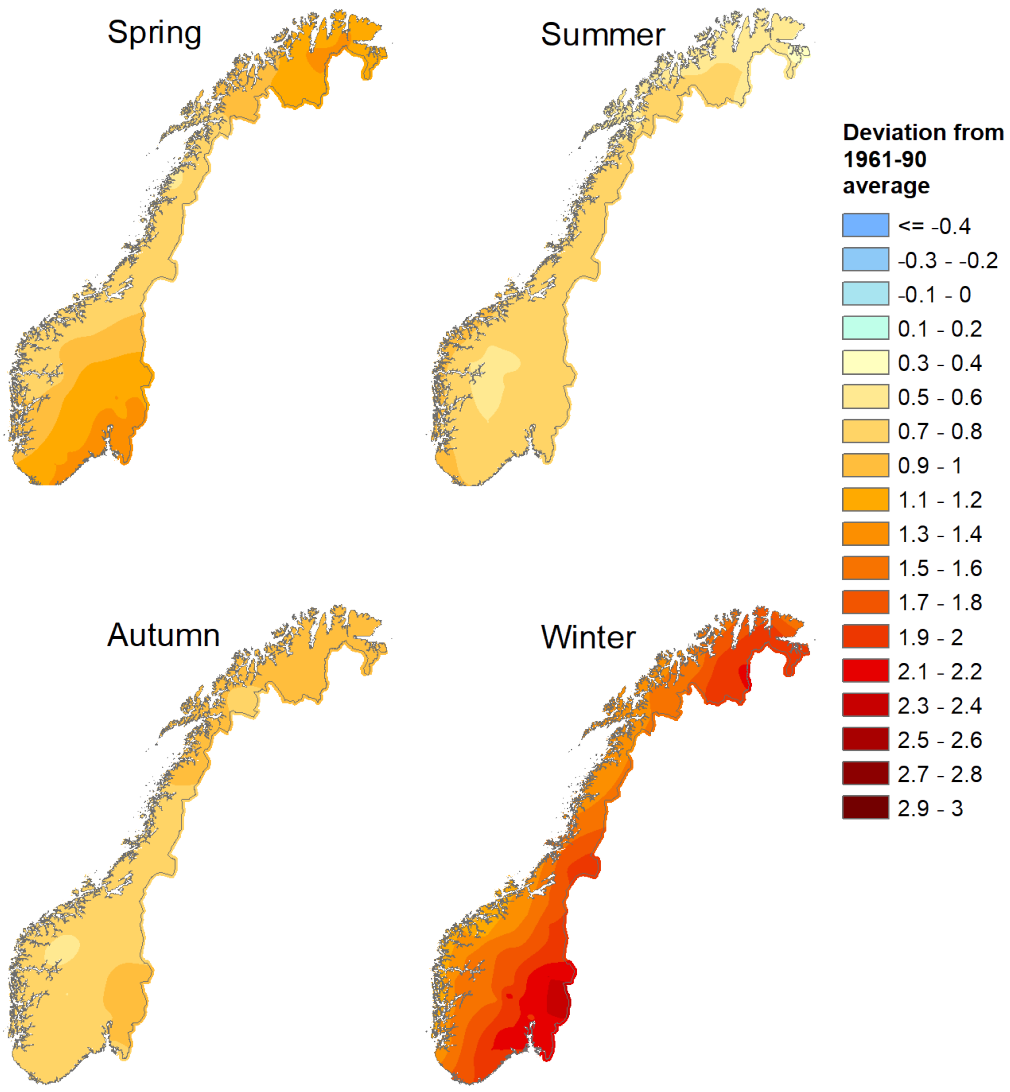

Figure 17: The difference between mean seasonal temperatures in the period 1991-2020 and the period 1961-1990.

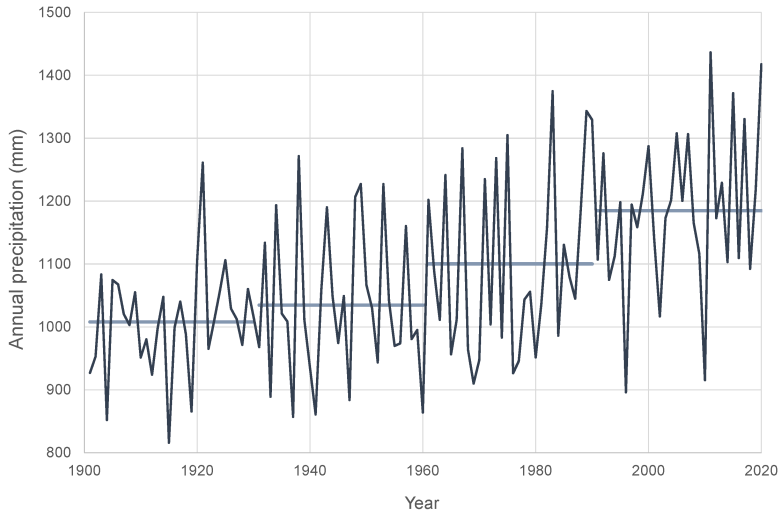

Figure 18: Average mean annual precipitation in Norway 1901-2020. The horizontal lines represent the consecutive 30 year average (normal) values 1901-1930,1931-60, 1961-90 and 1991-2020.

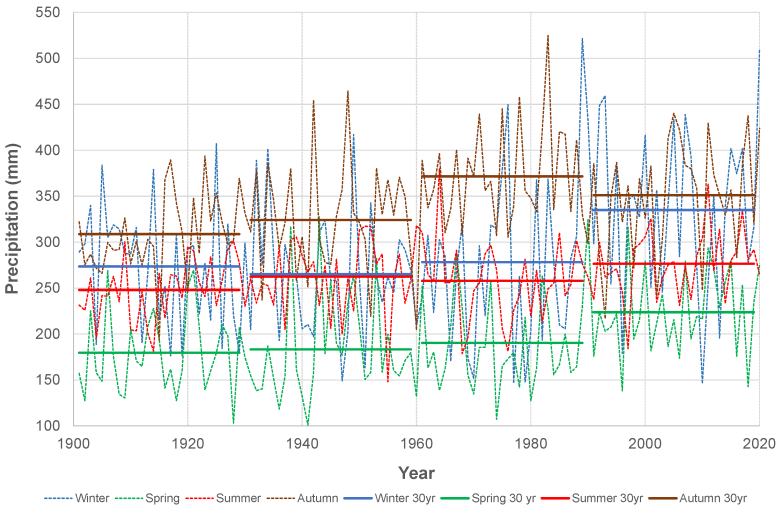

Figure 19: Average mean seasonal precipitation in Norway 1901-2020. The horizontal lines represent the consecutive 30 year average (normal) values 1901-1930,1931-60, 1961-90 and 1991-2020.

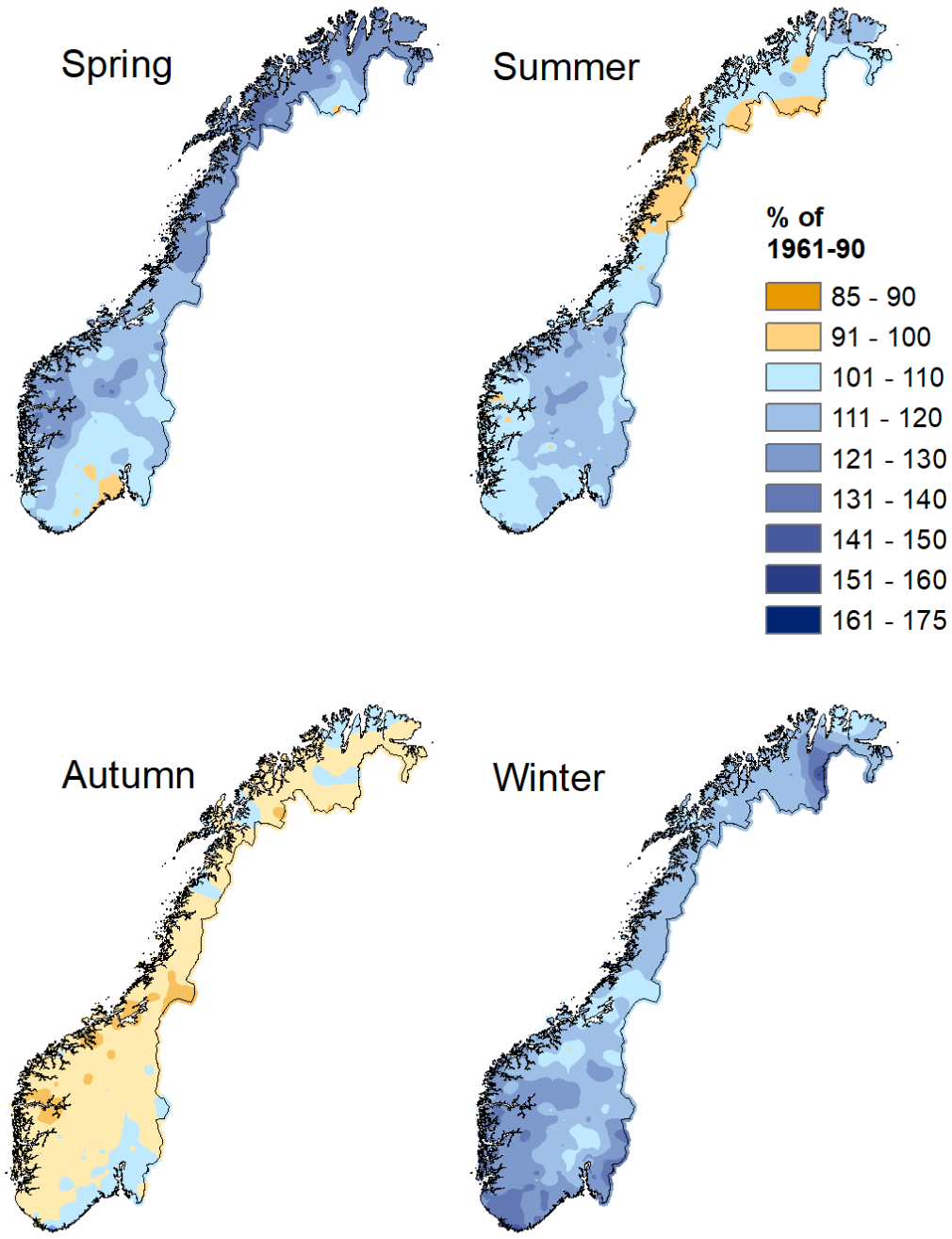

Figure 20: The ratio (in %) between mean seasonal precipitation in the period 1991-2020 and the period 1961-1990.

Akcnowledgements

The author wants to thank his colleagues Elinah Khasandi Kuya, Herdis Motrøen Gjelten, Inger Hanssen-Bauer, Lars Grinde and Cristian Lussana for assistance, discussions and helpful and critical comments while doing the analyses and preparing this report.

References

Alexandersson, H. (1986), A homogeneity test applied to precipitation data, *Journal of Climatology*, *6*(6), 661–675, doi:10.1002/joc.3370060607.

Aune, B. (1993), Temperturnormaler, normalperiode 1961-1990, *DNMI-Rapport*, *02/79 Klima*.

Domonkos, P. (2019), The ACMANTv4 software package the ACMANTv4 software package, *Tech. rep.*, Available at: https://github.com/dpeterfree/ACMANT.

Førland, E. J. (1979), Nedbørens høydeavhengighet (precipitation and topography), *KLIMA*, *02/79*, 3–23.

Førland, E. J. (1993), Nedbørnormaler, normalperiode 1961-1990), *DNMI-rapport*, *29/93 Klima*.

Guijarro, J. (2018), Homogenizaton of climatic timeseries with climatol, version 3.1.1, *Tech. rep.*, doi:10.13140/RG.2.2.27020.41604.

Hutchinson, M. F. (1989), A new procedure for gridding elevation and stream line data with automatic removal of spurious pits, *Journal of Hydrology*, *106*, 211–232.

Kuya, E. K., H. M. Gjelten, and O. E. Tveito (2020), Homogenization of Norway's mean monthly temperature series, *METreport*, *03/20 Climate*.

Kuya, E. K., H. M. Gjelten, and O. E. Tveito (2021), Homogenization of Norwegian monthly precipitation series for the period 1961-2018, *METreport*, *04/21 Climate*.

Lussana, C., O. E. Tveito, A. Dobler, and K. Tunheim (2019), senorge_2018, daily precipitation, and temperature datasets over norway, *Earth System Science Data*, *11*(4), 1531–1551, doi:10.5194/essd-11-1531-2019.

Mestre, O., P. Domonkos, F. Picard, I. Auer, S. Robin, E. Lebarbier, R. Böhm, E. Aguilar, J. A. Guijarro, G. Vertacnik, et al. (2013), HOMER: a homogenization software–methods and applications.

Press, W., S.A.Teukolsky, W.T.Vetterling, and B. Flannery (1992), *Numerical Recipes in Fortran*, Cambridge University Press.

Tveito, O., E. Førland, R. Heino, I. Hanssen-Bauer, H. Alexandersson, B. Dahlström, A. Drebs, C. Kern-Hansen, T. Jónsson, E. Vaarby Laursen, et al. (2000), Nordic temperature maps, *DNMI report*, *9/00 Klima*.

Tveito, O., E. Førland, H. Alexandersson, A. Drebs, T. Jónsson, H. Tuomenvirta, and V. L. E (2001), Nordic climate maps, *DNMI report*, *6*(00).

Tveito, O. E., I. Bjørdal, A. O. Skjelvåg, and B. Aune (2005), A GIS-based agro-ecological decision system based on gridded climatology, *Meteorological Applications*, *12*(1), 57–68.

Wahba, G. (1990), Spline models for observational data, *Paper presented at CBMS-NSF Regional Conference Series in Applied Mathematics. Philadelphia: Soc. Ind. Appl. Maths.*

WMO (2017), WMO Guidelines on the Calculation of Climate Normals, *Tech. Rep. WMO-No. 1203*, World Meteorological Organization.

WMO (2018), Guide to Climatological Practices, *Tech. Rep. WMO-No. 100*, World Meteorological Organization.